ELSEVIER

Available online at www.sciencedirect.com

SCIENCE DIRECT®

Physics of the Earth and Planetary Interiors xxx (2003) xxx–xxx

PHYSICS OF THE EARTH AND PLANETARY INTERIORS

www.elsevier.com/locate/pepi

On the resolution of density within the Earth

Guy Masters [a,*], David Gubbins [b]

[a] *IGPP, SIO, UCSD, 9500 Gilman Drive, La Jolla, CA 92093-0225, USA*
[b] *School of Earth Sciences, University of Leeds, Leeds LS2 9JT, UK*

Accepted 11 July 2003

Abstract

Roughly 30 years have passed since the last publication of a linear resolution calculation of density inside the Earth. Since that time, the data set of free oscillation degnerate frequencies has been completely re-estimated taking into account the biassing effects of splitting and coupling due to 3D structure. This paper presents a new resolution analysis based on the new data and focuses on two particular issues: (1) the density jump at the inner-core boundary which is important in discussions of the maintenance of the geodynamo; and (2) a possible density excess in the lowermost mantle which might be indicative of a "hot abyssal layer". We find that the density jump at the inner-core boundary is $0.82 \pm 0.18\,\mathrm{Mg\,m^{-3}}$ which is significantly larger than previously thought. We also find little support for an excess density in the lowermost mantle though an increase of 0.4% is possible.

Keywords: Free oscillation; Biassing effects; Inner-core boundary(ICB)

1. Introduction

New calculations of the energy required to power the dynamo (Buffet et al., 1996; Labrosse et al., 1997; Stacey and Stacey, 1999; Gubbins et al., in press) suggest that there may be difficulty in maintaining a dynamo throughout earth history and that the inner-core of the Earth is a relatively young feature. It has long been known that an efficient way of maintaining the dynamo is by compositional convection associated with the growth of the inner-core (Loper, 1978; Gubbins et al., 1979). The amount of energy that this source can produce is critically dependent on the density jump at the inner-core boundary (ICB) (more correctly, on the percentage of the density jump which is associated with a compositional jump at the ICB). A larger density jump means that a dynamo can be maintained with slower growth rates of the inner-core than would otherwise be necessary. Another issue of considerable interest which requires an accurate knowledge of the density within the Earth is the possible existence of a compositionally distinct layer in the lower mantle. Such a layer has been proposed by Kellogg et al. (1999) as a repository for a variety of geochemical components including radioactive elements. Such a layer would be hot but would maintain a higher density than the mantle above because of a differing chemical composition. Kellogg et al. (1999) estimate that an excess density of about 1% (over an isochemical mantle) would result in a stable layer though with a strong topography on its upper boundary. This strong topography would make the layer difficult to detect using standard seismic techniques.

The density jump at the ICB can currently be constrained using two techniques. One relies on estimates

* Corresponding author. Fax: +1-858-534-5332.
E-mail address: guy@igpp.ucsd.edu (G. Masters).

0031-9201/$ – see front matter © 2003 Published by Elsevier B.V.
doi:10.1016/j.pepi.2003.07.008

of the impedance contrast at the ICB based on the amplitude of the reflected phase *PKiKP*. *PKiKP* is rarely observed and there is some concern that observations may only be possible when focusing gives unusually large amplitudes. Indeed, early work using this technique (Bolt and Qamar, 1970; Souriau and Souriau, 1989) suggested that the density jump may be as large as $1.6\,\mathrm{Mg\,m^{-3}}$ which is about three times the currently accepted value. Shearer and Masters (1990) evaluated these results and found that *PKiKP* should be observed much more often if the density jump really is this large. They gave an approximate upper limit of $1.0\,\mathrm{Mg\,m^{-3}}$. New measurements using high frequency seismic arrays may go some way to refining this estimate.

The second technique uses the fact that free oscillation frequencies are sensitive to density within the Earth. The last published general calculation of resolution of density was given by Gilbert et al. (1973) though Masters (1979) gave a discussion of how well the density jump at the ICB was resolved using a free oscillation data set compiled by Gilbert and Dziewonski (1975). Much of the original data set came from spectra of digitized recordings of a single earthquake—the 1970 Colombian event. Since that time, many great earthquakes have been recorded by the ever-expanding global digital seismic network allowing an extensive evaluation of the effect of 3D structure on free oscillation frequencies. This has resulted in a data set of extremely accurate degenerate frequencies for some 850 free oscillations, over 50of which sample the inner-core (see the Reference Earth Model web page for details:http://mahi.ucsd.edu/Gabi/rem.html). Of these 50, the radial modes provide some of the greatest sensitivity to density in the deep earth (Dahlen and Tromp, 1998).

Density resolution in the Earth using free oscillation frequencies has been recently discussed by Kennett (1998) who uses a non-linear technique. Computational considerations lead him to use a rather small subset of mode frequencies and he also assumed that the seismic velocities were known perfectly. In the next section, we present a standard *linear* resolution analysis using the full mode dataset with ascribed error bounds on the frequencies and taking into account uncertainties in the seismic velocities. This gives a good indication of the resolution available to us. Using the complete mode data set and allowing trade-offs between seismic velocity and density with the non-linear method is still computationally infeasible but should be kept in mind for the future.

2. A standard resolution analysis

A (fairly) straightforward application of perturbation theory relates a relative perturbation in the k'th mode degenerate frequency (ω_k) to perturbations in the radial profiles of seismic velocities and density as well as perturbations in the radii of discontinuities (h_j):

$$\frac{\delta\omega_k}{\omega_k} \pm \sigma_k = \int_0^a \left[K_k(r)\frac{\delta V_p}{V_p}(r) + M_k(r)\frac{\delta V_s}{V_s}(r) + R_k(r)\frac{\delta\rho}{\rho}(r) \right] \mathrm{d}r + \sum_j A_{jk}\delta h_j \qquad (1)$$

where the kernels (K, M, R, A_j) can be easily computed for each mode from the eigenfunctions of some reference model (Woodhouse and Dahlen, 1978; Dahlen and Tromp, 1998). Eq. (1) assumes that the reference model is linearly close to the real spherically averaged Earth which is a good approximation for most modes (though see below).

First, we perform a standard resolution analysis following Backus and Gilbert (1970). We attempt to construct a datum from a linear combination of all our free oscillations frequencies which is sensitive only to some property (e.g. density) concentrated about some target radius (r_0) . That is, we seek multipliers, a_k, such that

$$\sum_k a_k \frac{\delta\omega_k}{\omega_k} = \int_0^a \left[\mathcal{K}(r)\frac{\delta V_p}{V_p}(r) + \mathcal{M}(r)\frac{\delta V_s}{V_s}(r) + \mathcal{R}(r)\frac{\delta\rho}{\rho}(r) \right] \mathrm{d}r + \sum_j \mathcal{A}_j\delta h_j \qquad (2)$$

where $\mathcal{K} = \sum_k a_k K_k$, $\mathcal{M} = \sum_k a_k M_k$, $\mathcal{R} = \sum_k a_k R_k$, $\mathcal{A}_j = \sum_k a_k A_{jk}$. If we were trying to resolve density, we should choose the mulitpliers to make $\mathcal{R}$ as peaked as possible at the target radius and $\mathcal{K}, \mathcal{M}, \mathcal{A}_j$ are made as small as possible (preferably zero). In this case, $\mathcal{R}$ is called the "resolving kernel". Our linear combination of data will then be related to the average of density integrated over the resolving kernel (this is called the "local average" in Backus–Gilbert terminology). This local average is made unbiased by forcing the resolving kernel to be unimodular:

$$\boldsymbol{a}\cdot\boldsymbol{b}=1 \quad \text{where} \quad b_k=\int_0^a R_k\,\mathrm{d}r \tag{3}$$

Backus and Gilbert show that minimizing $\boldsymbol{a}\cdot\boldsymbol{S}\cdot\boldsymbol{a}$ with $\boldsymbol{S}$ given by

$$S_{ik}=\int_0^a [12R_iR_k(r-r_0)^2+M_iM_k+K_iK_k]\,dr + \sum_j A_{ji}A_{jk} \tag{4}$$

results in a resolving kernel of the desired shape. The factor of 12 in the above equation is chosen to make $\boldsymbol{a}\cdot\boldsymbol{S}\cdot\boldsymbol{a}$ (the "spread") a measure of the width of the resolving kernel. The spread can sometimes have a large contribution from the fact that the resoving kernel is not well-centered at the target radius—we therefore also calculate the "center" of the kernel and the spread about the center (called the "width") following the recipe given by Backus and Gilbert (1970).

When the data have errors, the linear combination on the left hand side of Eq. (2) will have an associated error. We would also like to choose the a_k's to minimize this error since it determines how precise our local average will be. Errors on the mode observations map to a contribution $\sigma_{\mathrm{av}}^2=\boldsymbol{a}\cdot\boldsymbol{E}\cdot\boldsymbol{a}$ where $\boldsymbol{E}$ is the covariance matrix of the observations (usually taken to be diagonal). Not surprisingly, the two goals of choosing a combination of data which isolates information about a property at some target radius and having that combination be precise are mutually exclusive and we have a trade-off between the two. In practice, we minimize $\boldsymbol{a}\cdot\boldsymbol{M}\cdot\boldsymbol{a}$ subject to $\boldsymbol{a}\cdot\boldsymbol{b}=1$ with $\boldsymbol{M}=\boldsymbol{S}+\lambda\boldsymbol{E}$. The solution is

$$\boldsymbol{a}=\frac{\boldsymbol{M}^{-1}\cdot\boldsymbol{b}}{\boldsymbol{b}\cdot\boldsymbol{M}^{-1}\cdot\boldsymbol{b}} \tag{5}$$

The trade-off parameter, λ, is varied until some desired value of σ_{av} is achieved.

Figs. 1–3 give the width as a function of the center of the kernel for various target error levels for density, shear velocity, and compressional velocity respectively. Fig. 4 illustrates the resolving kernel for density for a target σ_{av} of 0.5%. For compressional and shear velocity in the mantle, we can make acceptable resolving kernels for target error levels as small as 0.05% but this is not true for shear velocity in the inner-core or for density anywhere. If we ask for target levels much less than 0.5% for density, we typically end up with spreads greater than the radius of the Earth. On the

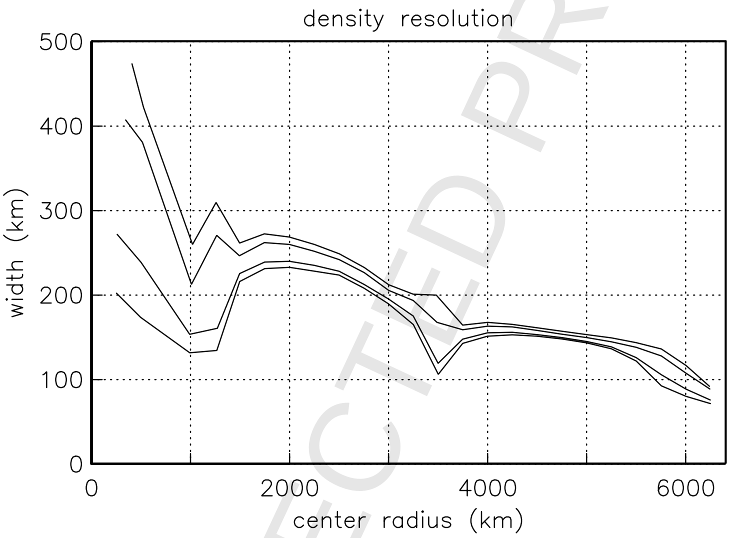

Fig. 1. Theoretical resolution of density in the Earth by the free-oscillation data set for various target error levels. Starting from the top curve, the target errors are 0.5, 1, 5, and 10%. As an example of how to read this plot, the density at a radius of 2000 km is known to an error of 0.5% if averaged over a resolving length of about 270 km.

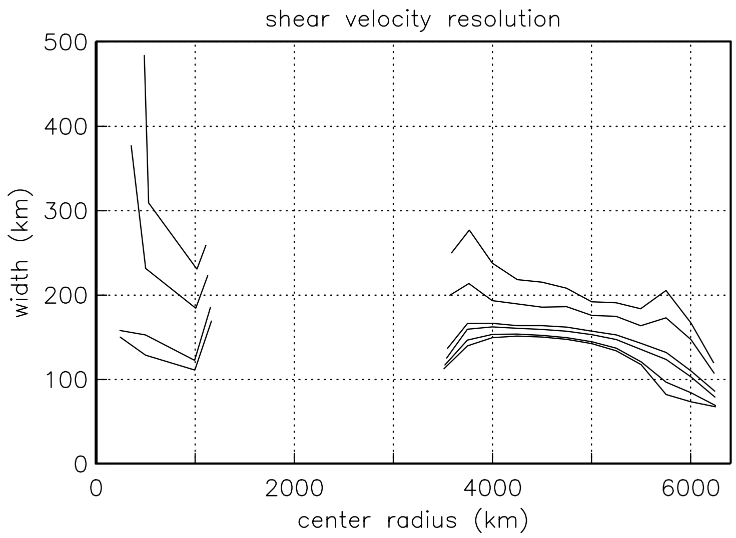

Fig. 2. Theoretical resolution of shear velocity in the Earth by the free-oscillation data set. The four curves in the inner-core are for target error levels of 0.5, 1, 5, and 10% (from top to bottom). In the mantle, there are six target error levels of 0.05%, 0.1%, 0.5%, 1%, 5%, and 10% (from top to bottom).

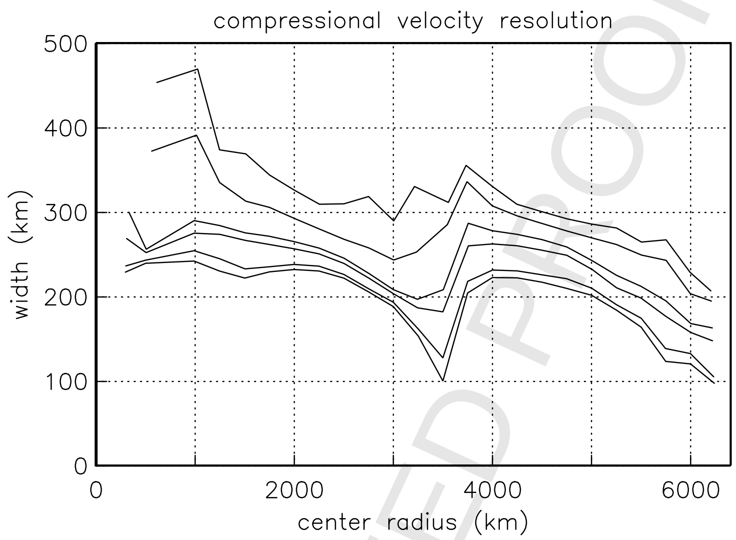

Fig. 3. Theoretical resolution of compressional velocity in the Earth by the free-oscillation data set. There are six target error levels of 0.05, 0.1, 0.5, 1, 5, and 10% (from top to bottom).

other hand, at 0.5%, density is resolved over widths as low as 150 km in the mantle, 250 km in the outer core, and about 400 km in the top of the inner-core.

These results indicate that the free oscillation data are capable of saying useful things about density in the inner-core and in the lowermost mantle.

3. A modified analysis

The careful reader will note that we have said nothing about the actual density inside the earth—just about our ability to resolve it. If we wish to use Eq. (1) to make quantitative statements about density,

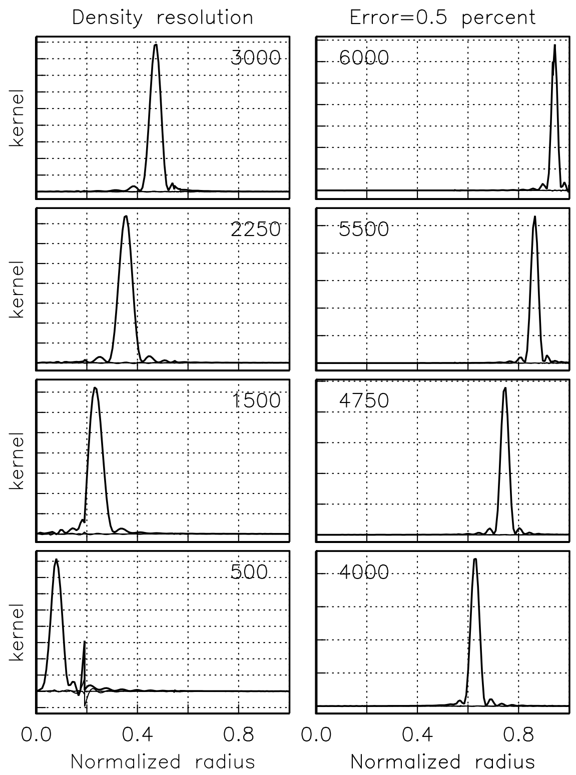

Fig. 4. Resolving kernels for density for a target error level of 0.5% and for various target radii. The heavy curve is $\mathcal{R}$ while the light curves (close to zero and not always visible) are $\mathcal{M}$ and $\mathcal{K}$.

we have to be sure that certain conditions are fulfilled. The primary condition is that the non-linear terms neglected in Eq. (1) can really be neglected. Clearly, this is not true for modes whose frequencies have been measured very precisely as even a small non-linear term is amplified by error weighting. After some experiment, we found Eq. (1) to be satisfactory if we force the observational errors to be greater than 0.05%. In effect, we are degrading the information available in the free oscillation data set but we gain the ability to do a linear analysis. Even at this level, a few mode frequencies can be strong non-linear functions of the starting model (this is true of modes whose eigenfunctions change from oscillatory to exponential behavior close to an internal discontinuity) and such modes have been removed from further analysis.

Another issue is the interpretation of "local averages" when the exact shape of the resolving kernel is not simple. We have found it easiest to make resolution kernels which are approximations to boxcars between specified radii (r_1, r_2), which we can achieve if we do not try to make $r_2 - r_1$ too small. The local average over the model computed with such a kernel can be compared with the true mean of the model between r_1 and r_2 and allows us to assess any bias. To make boxcar resolving kernels, it suffices to replace $\boldsymbol{S}$ in Eq. (1) by

$$S_{ik} = \int_0^a [R_i R_k + M_i M_k + K_i K_k]\,\mathrm{d}r + \sum_j A_{ji} A_{jk}$$

and $\boldsymbol{b}$ in Eq. (3) by

$$b_k = \int_{r_1}^{r_2} R_k\,\mathrm{d}r$$

The solution is again given by Eq. (5) (see equation 42 of Masters and Gilbert, 1983). If the data have been "ranked and winnowed" following the procedure of Gilbert (1971), S_{ij} will just be δ_{ij} and $\boldsymbol{M} = \boldsymbol{I} + \lambda \boldsymbol{E}$ is diagonal. Eq. (5) is then trivial to solve for a variety of λ's until a desired σ_{av} is achieved.

Suppose our minimization is successful in the sense that $\mathcal{K}, \mathcal{M}, \mathcal{A}_j$ are small enough to be neglected, then

$$\bar{\rho}_\mathrm{e} \simeq \bar{\rho}_\mathrm{m}\left(1 + \sum_k a_k \frac{\delta\omega_k}{\omega_k}\right) \tag{6}$$

where $\bar{\rho}_\mathrm{m}$ is the model density averaged between r_1 and r_2 and $\bar{\rho}_\mathrm{e}$ is our inferred local average for the real earth. σ_{av} is the relative error on $\bar{\rho}_\mathrm{e}$.

When $\mathcal{K}, \mathcal{M}, \mathcal{A}_j$, are not exactly zero, these terms can be thought of as contributing an additional uncertainty in the answer (this was called the "contamination" by Masters, 1979). We can make an upper estimate of the contamination by choosing maximum allowable perturbations in density and velocity as a function of radius (see e.g., Masters, 1979 for somewhat dated bounds) and computing terms such as

$$C_{Vp} = \int_0^a |\mathcal{K}| \left|\frac{\delta V_p}{V_p}\right|_{\max} \mathrm{d}r$$

The total contamination in a local average of density would then be given by

$$C = [C_{Vp}^2 + C_{Vs}^2 + C_h^2]^{1/2} \tag{7}$$

The total relative uncertainty on the local average is then bounded by $[\sigma_{av}^2 + C^2]^{1/2}$. Having said this, we will mainly confine attention to those solutions where the contamination is much less than the error due to observational uncertainty.

To test the validity of the assumptions behind our analysis, we computed a synthetic data set for a model with density in the inner-core increased by a rather extreme 10%. We were able to construct a resolving kernel which was a good approximation to a box car in the inner-core provided $\sigma_{av} \geq 1\%$ and recovered the correct mean density of the inner-core to within the observational uncertainty. Thus, equation (1) with data errors forced to be greater than 0.05% is linear to perturbations of at least 10%. As an additional test, we repeated the analysis to estimate the mean density in the inner-core using five different 1D models of the earth (1066A, 1066B of Gilbert and Dziewonski, 1975; PEMA of Dziewonski et al., 1975; isotropic PREM of Dziewonski and Anderson, 1981; AK135 of Montagner and Kennett, 1996). Despite the fact that these models fit the data to very different extents, the local average that is recovered is always independent of the starting model (within the observational uncertainty).

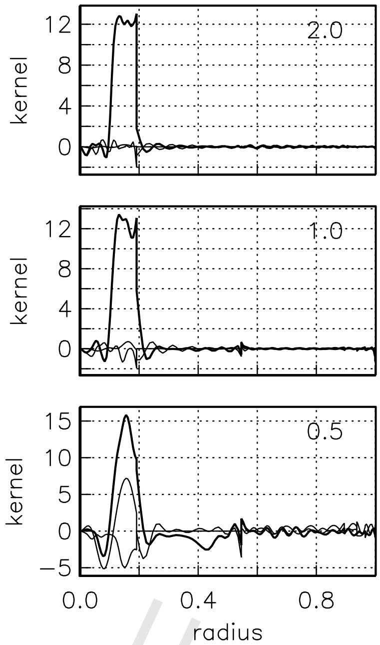

Fig. 5. Attempts to make a boxcar resolving kernel for density in the top 500 km of the inner-core for target error levels of 0.5, 1, and 2% (from bottom to top). The heavy curve is $\mathcal{R}$ while the light curves are $\mathcal{M}$ and $\mathcal{K}$. Contamination is significant for the 0.5% case reflecting the reduced sensitivity of the modes to structure near the center of the Earth. Using $\mathcal{R}$ in either of the top two cases to estimate the mean density of the model in this region (as opposed to a true boxcar) results in an error of less than 0.02%.

4. The density jump at the ICB

To estimate the density jump at the ICB, we consider two 500 km wide regions centered 250 km above and below the ICB. Fig. 5 shows resolving kernels for various target error levels for the region below the ICB. Clearly, a target of 0.5% leads to a rather poor resolving kernel (with significant contamination) but a target of 1% or greater gives a well-formed resolving kernel with very little contamination. At 1% error, the local averages for the five different models vary between 12.90 and 12.95 Mg m^{-3} with a median of 12.91 Mg m^{-3}. At 2%, the median local average for the five models is 13.07 Mg m^{-3}. Both of these numbers are slightly higher than the median of the model means which is 12.83 Mg m^{-3}. These results suggest that the modes prefer a slightly denser upper inner-core than usually found in 1D Earth models.

Resolving kernels for the region above the ICB are shown in Fig. 6. The 1% resolving kernel is not quite as flat as we would like but the bias induced by using this kernel instead of a true boxcar in estimating means is less than 0.05%. The local averages for the five models vary between 11.76 and 11.90 Mg m^{-3} with a median of 11.80 Mg m^{-3}. At 2%, the median local average is 11.71 Mg m^{-3}. Both of these numbers are slightly lower than the median of the model means which is 12.01 Mg m^{-3}. Apparently, the modes prefer a slightly less dense lower outer core than is usual in 1D models. To check this possibility, we estimate the mean density of the whole outer core. We can make an extremely good boxcar in the outer core for target errors of 0.5% or even less (Fig. 7). We find a mean density of 11.16 ± 0.06 Mg m^{-3} compared with the models which have a mean density of 11.24 Mg m^{-3}. Apparently, a slight decrease in density for the whole outer core is indicated.

These small changes have a significant impact on our estimate of the density jump at the ICB. For exam-

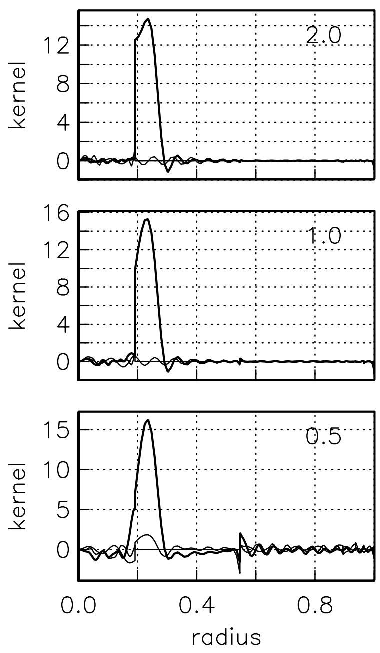

Fig. 6. Attempts to make a boxcar resolving kernel for density in the bottom 500 km of the outer core for target error levels of 0.5, 1, and 2% (from bottom to top). The heavy curve is $\mathcal{R}$ while the light curves are $\mathcal{M}$ and $\mathcal{K}$. Contamination is not totally negligible for the 0.5% case. Using $\mathcal{R}$ in either of the top two cases to estimate the mean density of the model in this region (as opposed to a true boxcar) results in an error of less than 0.04%.

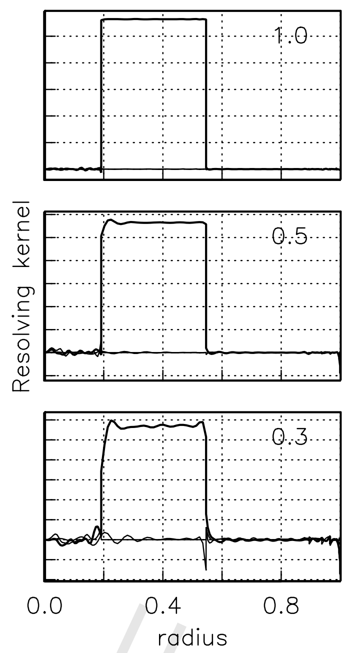

Fig. 7. Attempts to make a boxcar resolving kernel for density in the whole outer core for target error levels of 0.3, 0.5, and 1% (from bottom to top). The heavy curve is $\mathcal{R}$ while the light curves are $\mathcal{M}$ and $\mathcal{K}$. Using $\mathcal{R}$ in any of these cases to estimate the mean density of the model in the outer core (as opposed to a true boxcar) results in an error of less than 0.02%.

ple, the difference between the mean densities above and below the ICB in the starting models is on average 0.84 Mg m^{-3} of which 0.57 Mg m^{-3} comes from the density jump at the ICB and the other 0.27 Mg m^{-3} comes from compression effects (since we are dealing with means centered 250 km from the ICB). The compression contribution of 0.27 Mg m^{-3} agrees well with an estimate using the Adams–Williamson equation. On the other hand, the difference in the inferred local averages is 1.09 ± 0.18 Mg m^{-3} which leads to an inference of an inner core density jump of 0.82 ± 0.18 Mg m^{-3} (assuming a compression contribution of 0.27 Mg m^{-3}). The density jump due to solidification alone can be estimated to be about 0.21 Mg m^{-3} (Alfe et al., 2000; Gubbins et al., in press); so our new estimate increases the compositional part of the density jump from 0.36 to 0.62 Mg m^{-3}. The consequences of this for the thermal history of the core will be considered elsewhere.

5. The density near the base of the mantle

We now consider the bottom 500 km of the lower mantle. It should be noted that the models by and large closely follow the Adams–Williamson condition and show no signs of an unusual density increase near the base of the mantle. The exception is model AK135 which was constructed in an unusual way and has enhanced density in the bottom 150 km of the lower mantle. While it is true that this model provides by far the poorest fit to the mode data, it is still within the range of linearity since the local averages predicted using this model agree well with local averages predicted using other models.

The resolving kernels for various target error levels are shown in Fig. 8. Clearly, well-shaped kernels are available for all target levels above 0.5%. The median of the local averages for density at either the 0.5% or 1% level is 5.465 Mg m^{-3} and is known

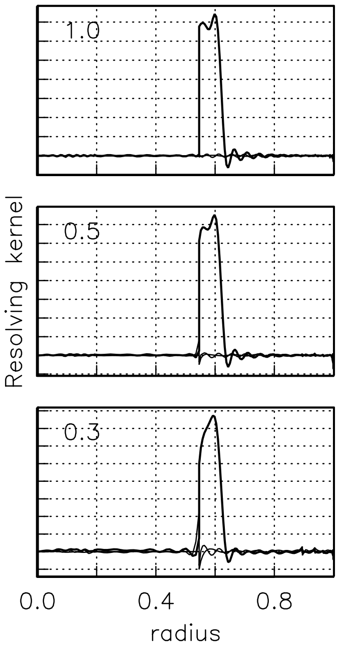

Fig. 8. Attempts to make a boxcar resolving kernel for density in the bottom 500 km of the lower mantle for target error levels of 0.3, 0.5, and 1% (from bottom to top). The heavy curve is $\mathcal{R}$ while the light curves are $\mathcal{M}$ and $\mathcal{K}$. Contamination is not totally negligible for the 0.3% case. Using $\mathcal{R}$ in either of the top two cases to estimate the mean density of the model in this region (as opposed to a true boxcar) results in an error of less than 0.05%.

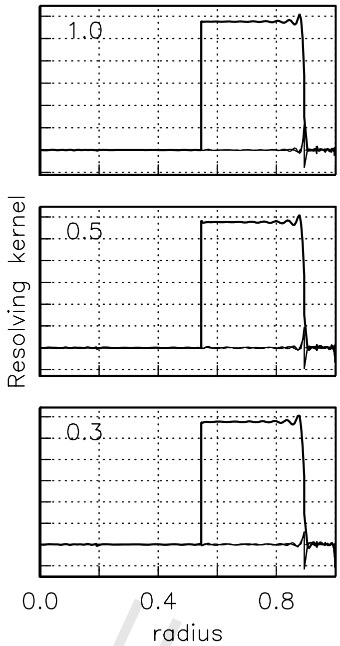

Fig. 9. Attempts to make a boxcar resolving kernel for density in the whole lower mantle (extending from the 660 km discontinuity to the core–mantle boundary) for target error levels of 0.3, 0.5, and 1% (from bottom to top). The heavy curve is $\mathcal{R}$ while the light curves are $\mathcal{M}$ and $\mathcal{K}$. Using $\mathcal{R}$ in any of these cases to estimate the mean density of the model in the lower mantle (as opposed to a true boxcar) results in an error of less than 0.03%.

to $\pm 0.027\,\mathrm{Mg\,m^{-3}}$. The median of the models is $5.447\,\mathrm{Mg\,m^{-3}}$ (though values range from 5.433 to $5.476\,\mathrm{Mg\,m^{-3}}$. These results imply that the bottom 500 km of the lower mantle may be about 0.4% more dense than the models though this difference is within the observational uncertainties.

We also computed resolving kernels for the mean density of the whole lower mantle (extending from the 660 km discontinuity to the core–mantle boundary). Not surprisingly, this can be done very accurately and we got good resolving kernels for target error levels of 0.3% (Fig. 9) leading to an estimate of mean lower mantle density of $4.996 \pm 0.015\,\mathrm{Mg\,m^{-3}}$ as compared to the models which had mean densities varying between 4.982 and $4.996\,\mathrm{Mg\,m^{-3}}$ with a median of $4.987\,\mathrm{Mg\,m^{-3}}$. This result implies that the whole lower mantle could be slightly denser than the models so the value of excess density in the lowermost mantle is likely to be less than 0.4%.

We believe these numbers put strong constraints on the likely viability of a “hot abyssal layer”. In Kellogg et al. (1999), a density constrast of 1% was cited after competing compositional and thermal effects were taken into account. Our results indicate that this may be too large by a factor of more than two. It should be remembered that this result was obtained for the degraded data set—non-linear inversions of the complete mode dataset should put even tighter constraints on possible excess density in the lowermost mantle.

6. Conclusions

We believe the results of this paper show that free oscillation degenerate frequencies are capable of constraining density in the Earth to a useful precision. The results of a linear analysis (with the errors on the mode frequencies degraded to ensure linearity) give a new estimate of the density jump at the ICB of $0.82 \pm 0.18\,\mathrm{Mg\,m^{-3}}$, which is significantly larger than the value used in previous calculations of the thermal history of the Earth's core. We also find that if, on average, the bottom 500 km of the lower mantle were acting as a "hot abyssal layer", its density excess would have to be less than 0.4%, which is about the observational uncertainty we have on density in this region. Whether such a layer would be dynamically stable remains to be seen.

Acknowledgements

This research was performed under NSF grant EAR01-12289 and under the DESMOND consortium funded by NERC grant NER/O/S/2001/006668. Guy Masters wishes to acknowledge discussions with Gabi Laske about the coupling effects on the radial mode degenerate frequencies.

References

Alfe, D., Kresse, G., Gillan, M.J., 2000. Structure and dynamics of liquid iron under Earth's core conditions. Phys. Rev. B 61, 132–142.

Backus, G.E., Gilbert, J.F., 1970. Uniqueness in the inversion of inaccurate gross earth data. Phil. Trans. R. Soc. Lond. A 266, 123–192.

Bolt, B.A., Qamar, A., 1970. Upper bound to the density jump at the boundary of the Earth's inner-core. Nature 228, 148–150.

Buffet, B.A., Huppert, H.E., Lister, J.R., Woods, A.W., 1996. On the thermal evolution of the Earth's core. J. Geophys. Res. 101, 7989–8006.

Dahlen, F.A., Tromp, J., 1998. Theoretical Global Seismology. Princeton University Press, Princeton, NJ.

Dziewonski, A.M., Anderson, D.L., 1981. Preliminary reference Earth model. Phys. Earth Planet Int. 25, 297–356.

Dziewonski, A.M., Hales, A.L., Lapwood, E.R., 1975. Parametrically simple earth models consistent with geophysical data. Phys. Earth Planet Inter. 10, 12–48.

Gilbert, F., 1971. Ranking and winnowing gross earth data for inversion and resolution. Geophys. J. R. Astronut. Soc. 23, 125–128.

Gilbert, F., Dziewonski, A.M., 1975. An application of normal mode theory to the retrieval of structural parameters and source mechanisms from seismic spectra. Phil. Trans. R. Soc. Lond. A 278, 187–269.

Gilbert, F., Dziewonski, A.M., Brune, J.N., 1973. An informative solution to a seismological inverse problem, Proc. Natl. Acad. Sci. 70, 1410–1413.

Gubbins, D., Masters, T.G., Jacobs, J.A., 1979. Thermal evolution of the Earth's core. Geophys. J. R. Astronut. Soc. 59, 57–99.

Gubbins, D., Alfe, D., Masters, G., Price, D., Gillan, M.J. Can the Earth's dynamo run on heat alone? Geophys. J. Int., in press.

Kellogg, L.H., Hager, B.H., van der Hilst, R., 1999. Compositional stratification in the deep mantle. Science 283, 1881–1884.

Kennett, B.L.N., 1998. On the density distribution within the Earth. Geophys. J. Int. 132, 374–382.

Labrosse, S., Poirier, J.-P., LeMouel, J.-L., 1997. On cooling of the Earth's core. Phys. Earth Planet Int. 99, 1–17.

Loper, D.E., 1978. Some thermal consequences of a gravitationally powered dynamo. J. Geophys. Res. 83, 5961–5970.

Masters, G., 1979. Observational constraints on the chemical and thermal structure of the earth's deep interior. Geophys. J. R. Astronut. Soc. 57, 507–534.

Masters, G., Gilbert, F., 1983. Attenuation in the earth at low frequencies. Phil. Trans. R. Soc. Lond. A 308, 479–522.

Montagner, J.-P., Kennett, B.L.N., 1996. How to reconcile body-wave and normal-mode reference Earth models. Geophys. J. Int. 125, 229–248.

Shearer, P.M., Masters, G., 1990. The density and shear velocity contrast at the inner-core boundary. Geophys. J. Int. 102, 491–498.

Souriau, A., Souriau, M., 1989. Ellipticity and density at the inner-core boundary from sub-critical *PKiKP* and *PcP* data. Geophys. J. 98, 39–54.

Stacey, F.D., Stacey, C.H.B., 1999. Gravitational energy of core evolution: implications of thermal history and geodynamo power. Phys. Earth Planet Int. 110, 83–93.

Woodhouse, J.H., Dahlen, F.A., 1978. The effect of a general aspherical perturbation on the free oscillations of the earth. Geophys. J. R. Astronut. Soc. 53, 335–354.